Hindawi
Advances in Materials Science and Engineering
Volume 2017, Article ID 3176808, 6 pages
https://doi.org/10.1155/2017/3176808

Research Article

Evaluating Mechanical Properties of Few Layers MoS_2 Nanosheets-Polymer Composites

Muhammad Bilal Khan, Rahim Jan, Amir Habib, and Ahmad Nawaz Khan

School of Chemical and Materials Engineering (SCME), National University of Sciences and Technology (NUST), H-12 Campus, Islamabad 44000, Pakistan

Correspondence should be addressed to Rahim Jan; rahimjan@scme.nust.edu.pk

Received 21 May 2017; Revised 22 July 2017; Accepted 3 August 2017; Published 10 September 2017

Academic Editor: Mikhael Bechelany

The reinforcement effects of liquid exfoliated molybdenum disulphide (MoS_2) nanosheets, dispersed in polystyrene (PS) matrix, are evaluated here. The range of composites (0~0.002 volume fraction (V_f) MoS_2-PS) is prepared via solution casting. Size selected MoS_2 nanosheets (3~4 layers), with a lateral dimension ⟨L⟩ 0.5~1 μm, have improved Young's modulus up to 0.8 GPa for 0.0002 V_f MoS_2-PS as compared to 0.2 GPa observed for PS only. The ultimate tensile strength (UTS) is improved considerably (~ ×3) with a minute addition of MoS_2 nanosheets (0.00002 V_f). The MoS_2 nanosheets lateral dimension and number of layers are approximated using atomic force microscopy (AFM). The composites formation is confirmed using X-ray diffraction (XRD) and scanning electron microscopy (SEM). Theoretical predicted results (Halpin-Tsai model) are well below the experimental findings, especially at lower concentrations. Only at maximum concentrations, the experimental and theoretical results coincide. The high aspect ratio of MoS_2 nanosheets, homogeneous dispersion inside polymer, and their probable planar orientation are the possible reasons for the effective stress transfer, resulting in enhanced mechanical characteristics. Moreover, the micro-Vickers hardness (H_V) of the MoS_2-PS is also improved from 19 (PS) to 23 (0.002 V_f MoS_2-PS) as MoS_2 nanosheets inclusion may hinder the deformation more effectively.

1. Introduction

The experimental discovery of graphene, due to its superior mechanical, electrical, thermal, and optical properties, has generated enormous interest in the field of polymer nanocomposites (PNCs) [1]. Graphene holds the best achieved mechanical characteristics with Young's modulus (Y) in the range of ~1 TPa and ultimate tensile strength (UTS) around 130 GPa [2]. The electrical properties are no less amazing with zero band gap, very high carrier mobility (~2×10^5 cm^2/Vs at room temp.), and electrical conductivity (~10^4 – 10^8 S/cm) [3]. With graphene, a surge in 2D materials followed a diverse range of materials with hexagonal boron nitride (hBN) and molybdenum disulphide (MoS_2) to be the other most followed layered materials. While hBN is electrically insulating, MoS_2 is semiconducting. The direct band gap of around 1.8 eV along with carrier mobility of ~200 cm^2/Vs for monolayer MoS_2 makes it go to material for switching and optoelectronics applications [4]. The in-plane stable structure of 2D materials is common among all, whether graphene, hBN, or MoS_2. The in-plane stability is mostly responsible for the extraordinary mechanical characteristics of graphene which are utilized extensively in PNCs. Other 2D materials like hBN and MoS_2 have been underutilized for reinforcement purpose; especially MoS_2, which has not been specifically assessed for its reinforcements effects in PNCs. Various research groups have tried to simulate as well as experimentally find Young's modulus and strength of single layer MoS_2. By using molecular dynamic simulations, Jiang et al. [5] predicted that the in-plane "Y" ~230 GPa which is compromised considering the "Y" for bulk MoS_2 is ~240 GPa. The thickness of single layer MoS_2 is around 6.092197 Å. Castellanos-Gomez et al. have experimentally studied the few layers (5–25) MoS_2 elastic deformations by utilizing atomic force microscope (AFM) bend tests. The "Y" ~330 ± 70 GPa, measured here, is very high and only one-third to "Y" of graphene (1 TPa) while considerably higher than graphene oxide, hBN, and bulk MoS_2 [6]. Bertolazzi et al. found the

in-plane stiffness of single layer MoS_2 ~270 ± 100 GPa along with the average breaking strength to be ~23 GPa [7]. These results show that few layer MoS_2 can be employed effectively for the reinforcement purpose as well as an alternating option to graphene in flexible electronics applications [8, 9].

Recently, the mechanical properties of the polyimide (PI) were improved considerably by a slight addition of MoS_2 nanosheets. Both the strength and "Y" were enhanced by 43% and 47%, respectively, at 0.75 wt% MoS_2 [10]. In another work, chemically modified 4 wt% MoS_2-polyurethane composites showed an increment of 140% and 85% in strength and "Y," respectively [11]. Same reinforcement effects have been observed for chitosan with strength being improved to 200% for 0.5 wt% MoS_2 [12]. The trend for utilizing MoS_2 as reinforcing filler is very compromised in comparison to graphene and graphene oxide. One possible reason may be the lack of high yield production of 2D nanosheets required for PNCs. Coleman group has been able to produce large quantities of defect-free 2D nanosheets with their famous liquid phase exfoliation method [13]. Here in this work we have prepared few layer MoS_2 via Coleman method of liquid phase exfoliation and dispersed in polystyrene matrix at various volume fractions (V_f) ranging from 0 to 0.002 V_f. The tensile properties of MoS_2-PS composites are measured as a function of MoS_2 V_f. The enhanced Young's modulus is evaluated based on two different theoretical models. We report the highest degree of reinforcement ($dY/dV_f \sim 320$) GPa for MoS_2 based polymer composites. The ultimate tensile strength and micro-Vickers hardness of MoS_2-PS composites are also enhanced.

2. Experimental Methods

As supplied MoS_2 (avg. grain size 6 μm), tetrahydrofuran (THF ≥ 99.9%), 1-methyl-2-pyrrolidinone (≥99.7%), and polystyrene (avg. molecular weight (MW): 35000) used in the work were purchased from Aldrich. MoS_2 was exfoliated in 1-methyl-2-pyrrolidinone solvent (20 mg/ml) by using ultrasonication. The probe sonicator (Model: UP50H, 50 watts, 30 kHz) was run at 0.3 cycle and 40% amplitude for 60 hrs at 2°C. After sonication, centrifugation was carried out (500 rpm for 90 min) to size select the exfoliated MoS_2 (by taking out the supernatant) and to remove any unexfoliated material. The supernatant was filtered out using nylon membrane (pore size ~ 0.4 μm) and dried at 120°C for 24 hrs. Solution processing method was used for the fabrication of polymer nanocomposites. Both MoS_2 (exfoliated) and PS were dispersed in THF with concentrations of 5 mg/ml and 50 mg/ml, respectively. A range of composites were prepared by taking dispersions from both filler and polymer solutions. The composite solutions were bath sonicated for 4 hrs to ensure the homogenous dispersions. The composite dispersions were poured in to Teflon molds. The solvent is evaporated at room temperature for 24 hrs followed by the vacuum drying at 65°C for 72 hrs. Tensile testing was performed using a Shimadzu tensile tester at a strain rate of 5 mm/min. The dimensions of samples (3–5) for each concentration were ~20 mm in length and ~10 mm in width while the thickness was around 0.05~0.06 mm.

3. Results and Discussion

The main aspect of liquid phase exfoliation of 2D nanosheets lies in the size selection. Ultracentrifugation at various rpm plays a vital role with a basic principal of continually changing the centrifugation speed from higher to lower range and getting the subsequent lower to higher aspect ratio nanosheets [14–17]. The lateral dimension of nanosheets (L) and number of layers per nanosheet (N) can be measured by utilizing Raman spectroscopy, transmission electron microscopy (TEM), and atomic force microscopy (AFM) [18]. Here in this work we have used AFM to estimate the "L" and "N" of MoS_2 nanosheets. Few drops of the MoS_2/THF were dropped onto the silicon substrate and scanned by utilizing AFM (Jeol SPM 5200) in tapping mode [19]. The average lateral dimension is around 0.5~1 micron while the number of layers is around 3~5. These are the average values based on the number of micrographs; a representative AFM image is shown as Figure 1(a). These values are highly approximated but give an indication about the exfoliation state of MoS_2. For lateral dimension consideration, scanning electron micrograph is shown in Figure 1(b), supporting the AFM approximations particularly for lateral dimension. The formation of MoS_2-PS composites and their crystalline phases were determined with the help of well-established X-ray diffraction (XRD) technique. Powder X-ray diffractometer is used having CuKα (1.54060 Å) as a source of radiation operated (40 mA and 40 kV) at room temperature and 2-theta (θ) ~ 5°–25°. The amorphous peak of PS appears around $2\theta \sim 21.3°$, while for MoS_2 the main peak is clearly visible at $2\theta \sim 14.4°$ shown in Figure 2. The strong $2\theta \sim 14.4°$[002] peak indicates a well-stacked layered structure for MoS_2 [20]. In composite state both polymer and filler peaks are retained at the same positions. Tensile testing results; Young's modulus (Y); and ultimate tensile strength (UTS) are shown in Figures 3(a)-3(b). Strain at break shows an improvement, but considering the error bar it remains constant up to 0.002 V_f MoS_2. Young's modulus, on the other hand, increases as a function of MoS_2 concentration and reaches up to maximum (0.84 GPa) at 0.0002 V_f MoS_2 as compared to the PS (0.21 GPa) shown in Figure 3(a). Beyond this loading (0.0002 V_f MoS_2), "Y" decreases a bit but remains constant ~0.6 GPa up to maximum loading (0.002 V_f MoS_2). The degree of reinforcement, dY/dV_f, is an indicator utilized for the filler effect on the outcome of PNCs mechanical characteristics [21]. The slope seems to be peaking at 0.0002 V_f MoS_2, but the error bar is large enough to consider the whole range of MoS_2 concentration for degree of reinforcement. Theoretical explanation for reinforcement can be done based on modified rule of mixtures (MRoM), expressed as [22]

$$Y_C = (\eta\eta_0 Y_F - Y_M) V_f + Y_M. \quad (1)$$

In the above equation, Y_C, Y_F, Y_M, and V_f represent Young's modulus of the composite, filler, polymer matrix, and volume fraction of filler, respectively. The length efficiency factor is

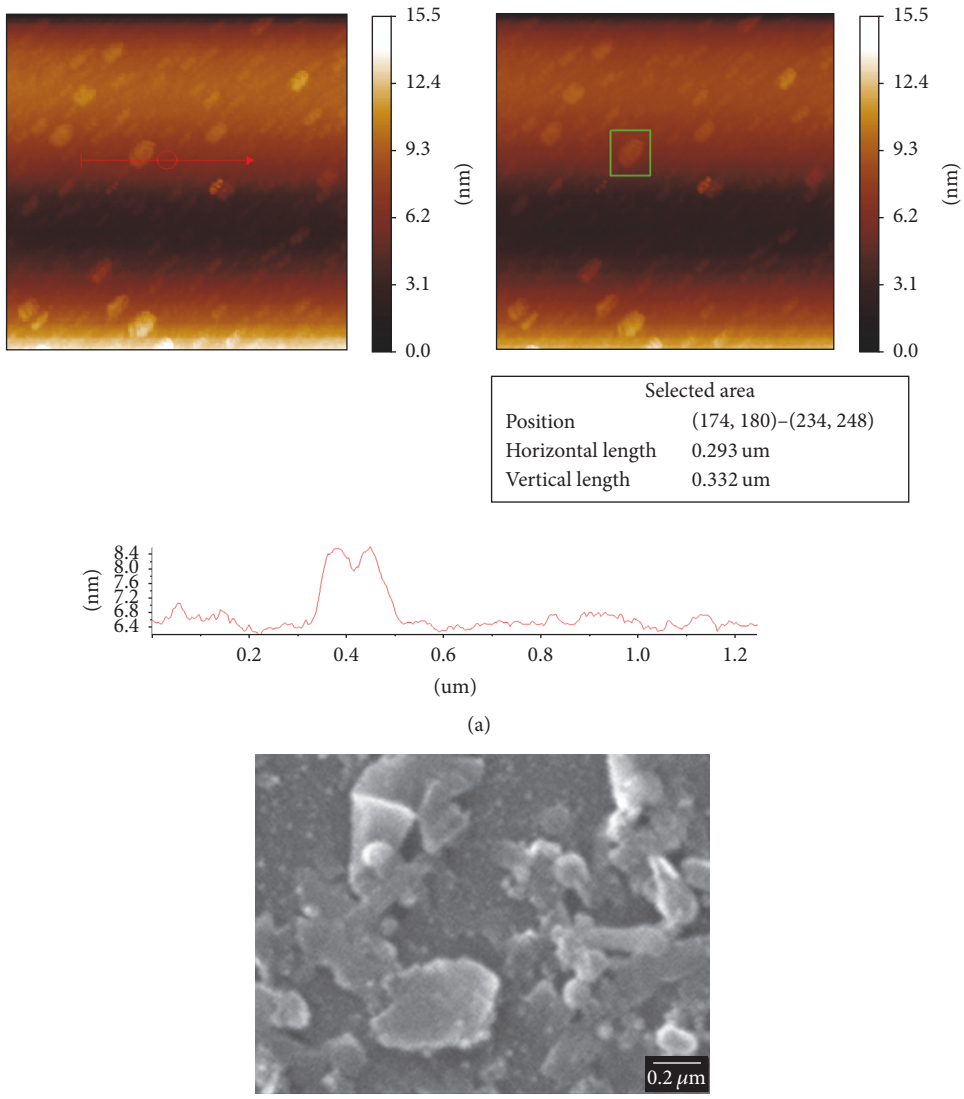

Figure 1: (a) Representative AFM image and dimensional analysis for MoS_2 nanosheets length (L) and number of layers (N). (b) Scanning electron micrograph of exfoliated MoS_2 for lateral dimension approximation.

depicted by η, evaluating the matrix-filler stress transfer effect [23].

$$\eta\,(\mathrm{MRoM}) = 1 - \frac{\tanh\,(nL/t)}{nL/t} \qquad \therefore n = \sqrt{\frac{G_P V_f}{Y_F\left(1 - V_f\right)}}. \quad (2)$$

The length efficiency factor depends on the filler aspect ratio (L/t) and Young's modulus (Y_F) along with the shear modulus of polymer matrix (G_P). The shear modulus of PS is calculated to be 0.078 by using the relationship $Y_P = 2G_P(1 + \upsilon)$, where υ is the Poisson ratio of PS. Another term in the above-mentioned MRoM expression is η_0, termed as orientation efficiency factor. Generally, 2D materials are randomly oriented in the polymer matrices, having orientation parameter ~0.38 [21]. The filler aspect ratio is an important parameter which can be utilized for estimation Y_C as shown above (see (2)). Both length and thickness of MoS_2 are estimated with AFM. The length is considered ~1 μm while thickness is ~2 nm. Analyzing the present scenario based on MRoM model, the experimentally found Young's modulus value of 0.213 GPa for PS is used. Young's modulus value for MoS_2 is 330 GPa [6, 8]. Overestimating both orientation parameter and length of MoS_2 to be in the range of 0.5~1 and ~2 μm, respectively, still the estimated theoretical Y_C from the MRoM model underestimates Young's modulus of these composites as shown in Figure 3(a). Another approach to predict Young's modulus as a function of filler volume fraction is Halpin-Tsai model. This model can particularly be

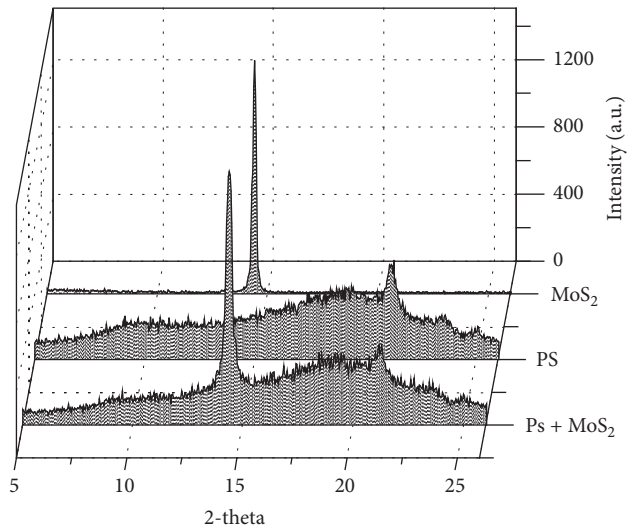

Figure 2: XRD results of PS, MoS_2, and MoS_2-PS composite.

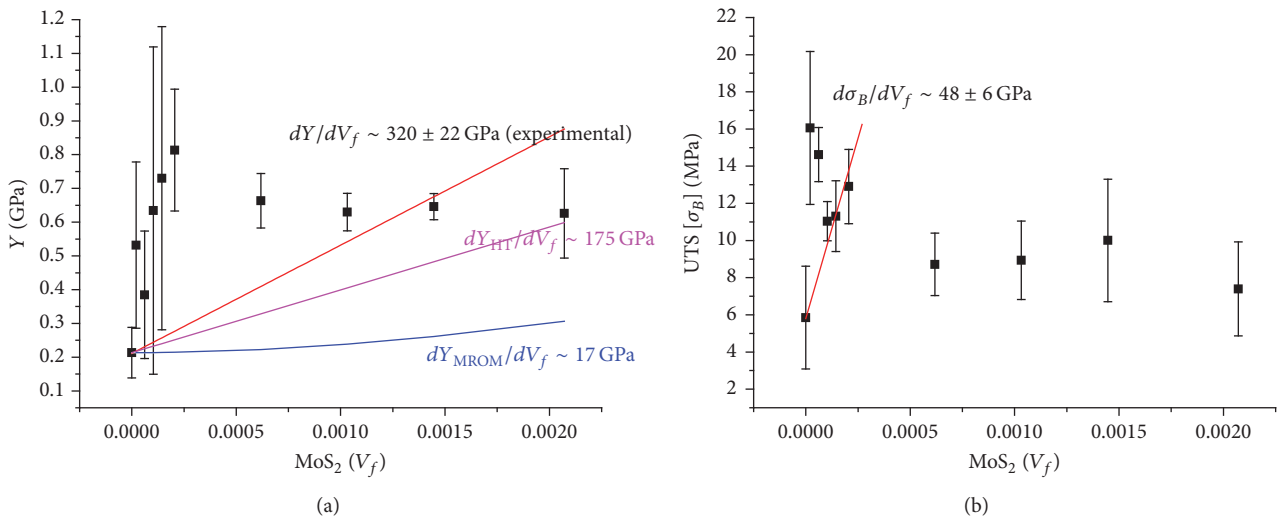

Figure 3: Modulus and ultimate tensile strength of MoS_2-PS composites as a function of MoS_2 volume fraction.

used for the well dispersed and aligned systems, expressed as under [21–23]

$$Y_C = Y_M \left[\frac{1 + 2V_f \eta L/t}{1 - V_f \eta} \right], \tag{3}$$

where

$$\eta\,(\mathrm{HT}) = \frac{Y_F/Y_M + 1}{Y_F/Y_M + 2L/t}. \tag{4}$$

Applying (3) to MoS_2-PS composites, the Halpin-Tsai modelled reinforcement is shown in Figure 3(a). The estimated theoretical results come close to the experimental results, especially when the overestimated MoS_2 length (2 μm) is used. But still these values are compromised as compared to the experimental findings. The rate of increase of Young's modulus (dY/dV_f) is a clear indicator of the reinforcement trend. The slope (dY/dV_f) of the H-T model is in the range 175 GPa while the experimental dY/dV_f ~ 320 ± 22 GPa (red line) shown in Figure 3(a). The Halpin-Tsai model predicts relatively better than MRoM as the main difference is reported to be in the dissimilar scaling behavior of the length efficiency factor. The experimental dY/dV_f ~320 GPa is almost equal to the few layer (5~25) MoS_2 in-plane stiffness (~330 ± 70 GPa) measured by Castellanos-Gomez et al. [6, 8]. The reason for such reinforcement (dY/dV_f ~ 320 GPa) of MoS_2-PS composites may be the improved dispersion of filler inside polymer, filler alignment, and strong interface between filler and polymer. It would be of great interest if these composites are drawn and then characterized for degree of reinforcement as was done for graphene and hBN based PNCs [19, 21]. UTS of the PS is enhanced considerably with a slight addition of MoS_2 as shown in Figure 3(b). The polymer only sample, when tested for UTS, reached around 4 MPa.

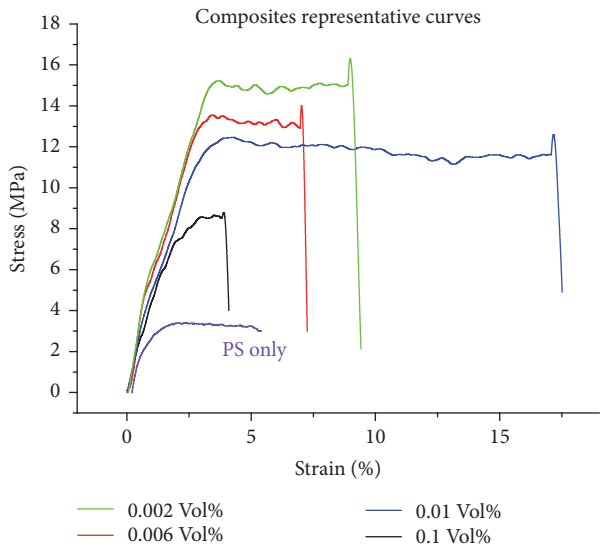

FIGURE 4: Representative stress-strain curves for the MoS_2-PS composites.

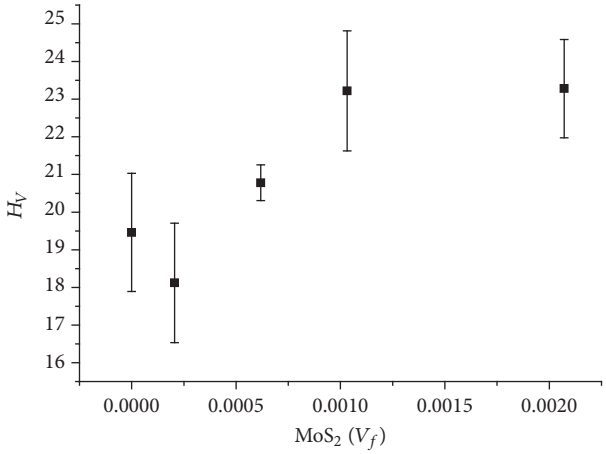

FIGURE 5: Hardness results for MoS_2-PS composites as a function of MoS_2 volume fraction.

By increasing MoS_2 concentration up to 0.0002 V_f, the UTS is well above 10 MPa and reaches up to ~16 MPa. Beyond 0.0002 V_f MoS_2 loading, the UTS decreases but remains around 8~10, well above the PS strength. Agglomeration may be adding up to the slight decrease in UTS at higher loading but seems that these aggregates are dispersed well for the overall effect. Interestingly $d(\sigma_B)/dV_f$ for MoS_2-PS composites is ~48 ± 6 GPa, almost doubled to the measured value of breaking strength of MoS_2 which is 23 GPa found by Bertolazzi et al. [7]. The representative stress-strain curves for the MoS_2-PS composites in various concentrations are shown in Figure 4. Hardness test was carried out with the help of digital Brinell hardness tester (Model: SHB3000C). Maximum increase in hardness value was up to 23.28 H_V at 0.001 V_f MoS_2 concentration as compared to 19.46 H_V of PS matrix as shown in Figure 5. The reason of increase in hardness value is presence of 2D layered structure present inside in composite phase. The reinforcement properties will be of great use for the further utilization of these free standing composite films/membranes. These mechanically robust composite films can be readily utilized for various applications like gas barrier properties and dielectric spectroscopy measurements and for filtration.

4. Conclusion

Liquid exfoliated, few layered, high aspect ratio MoS_2 nanosheets are dispersed in polystyrene matrix for reinforcement purpose. The degree of reinforcement is ~320 GPa, reaching up to the filler's Young's modulus (~330 GPa). The strength at break is also improved considerably as the rate of UTS as a function of MoS_2 volume fraction is around 48 GPa, twice the UTS of MoS_2 nanosheets. This work may lead to more utilization of MoS_2 nanosheets for the plastic reinforcement. Uniaxial drawing of MoS_2-polymer composites may also provide some more insight into the effect of aspect ratio and alignment inside composites.

Conflicts of Interest

The authors declare that they have no conflicts of interest.

References

[1] R. Jan, A. Habib, and I. H. Gul, "Stiff, strong, yet tough free-standing dielectric films of graphene nanosheets-polyurethane nanocomposites with very high dielectric constant and loss," *Electronic Materials Letters*, vol. 12, no. 1, pp. 91–99, 2016.

[2] C. Lee, X. Wei, J. W. Kysar, and J. Hone, "Measurement of the elastic properties and intrinsic strength of monolayer graphene," *Science*, vol. 321, no. 5887, pp. 385–388, 2008.

[3] X. Huang, X. Qi, F. Boey, and H. Zhang, *Chem. Soc. Rev*, vol. 41, pp. 666–686, 2012.

[4] X. Li and H. Zhu, *Journal of Materiomics*, vol. 1, pp. 33–44, 2015.

[5] J. W. Jiang, H. S. Park, and T. Rabczuk, *Journal of Applied Physics*, vol. 114, Article ID 064307, 2016.

[6] A. Castellanos-Gomez, M. Poot, G. A. Steele, H. S. J. Van Der Zant, N. Agraït, and G. Rubio-Bollinger, "Elastic properties of freely suspended MoS 2 nanosheets," *Advanced Materials*, vol. 24, no. 6, pp. 772–775, 2012.

[7] S. Bertolazzi, J. Brivio, and A. Kis, "Stretching and breaking of ultrathin MoS 2," *ACS Nano*, vol. 5, no. 12, pp. 9703–9709, 2011.

[8] A. Castellanos-Gomez, M. Poot, G. A. Steele, H. S. J. van der Zant, N. Agraït, and G. Rubio-Bollinger, "Mechanical properties of freely suspended semiconducting graphene-like layers based on MoS2," *Nanoscale Research Letters*, vol. 7, pp. 1–7, 2012.

[9] S. Bertolazzi, J. Brivio, A. Radenovic et al., *Microscopy and Analysis*, vol. 27, p. 21, 2013.

[10] H. Yuan, X. Liu, L. Ma et al., "Application of two-dimensional MoS2 nanosheets in the property improvement of polyimide matrix: Mechanical and thermal aspects," *Composites Part A: Applied Science and Manufacturing*, vol. 95, pp. 220–228, 2017.

[11] X. Wang, W. Xing, X. Feng et al., "Enhanced mechanical and barrier properties of polyurethane nanocomposite films with randomly distributed molybdenum disulfide nanosheets," *Composites Science and Technology*, vol. 127, pp. 142–148, 2016.

[12] X. Feng, X. Wang, W. Xing, K. Zhou, L. Song, and Y. Hu, "Liquid-exfoliated MoS2 by chitosan and enhanced mechanical and thermal properties of chitosan/MoS2 composites," *Composites Science and Technology*, vol. 93, pp. 76–82, 2014.

[13] K. R. Paton and etal., *Nature Materials*, vol. 13, pp. 623–630, 2014.

[14] U. Khan, A. O'Neill, H. Porwal, P. May, K. Nawaz, and J. N. Coleman, "Size selection of dispersed, exfoliated graphene flakes by controlled centrifugation," *Carbon*, vol. 50, no. 2, pp. 470–475, 2012.

[15] M. Lotya, P. J. King, U. Khan, S. De, and J. N. Coleman, "High-concentration, surfactant-stabilized graphene dispersions," *ACS Nano*, vol. 4, no. 6, pp. 3155–3162, 2010.

[16] A. O'Neill, U. Khan, and J. N. Coleman, "Preparation of high concentration dispersions of exfoliated MoS 2 with increased flake size," *Chemistry of Materials*, vol. 24, no. 12, pp. 2414–2421, 2012.

[17] P. May, U. Khan, A. O'Neill, J. N. Coleman, and J. Mater, *Chem*, vol. 22, pp. 1278–1282, 2012.

[18] C. Backes, K. R. Paton, D. Hanlon et al., "Spectroscopic metrics allow in situ measurement of mean size and thickness of liquid-exfoliated few-layer graphene nanosheets," *Nanoscale*, vol. 8, no. 7, pp. 4311–4323, 2016.

[19] R. Jan, A. Habib, M. A. Akram, T.-U. Zia, and A. N. Khan, "Uniaxial Drawing of Graphene-PVA nanocomposites: improvement in mechanical characteristics via strain-induced exfoliation of graphene," *Nanoscale Research Letters*, vol. 11, no. 1, article 377, pp. 1–9, 2016.

[20] G. Du, Z. Guo, S. Wang, R. Zeng, Z. Chen, and H. Liu, *Chem. Commun*, vol. 46, pp. 1106–1108, 2010.

[21] R. Jan, P. May, A. P. Bell, A. Habib, U. Khan, and J. N. Coleman, "Enhancing the mechanical properties of BN nanosheet-polymer composites by uniaxial drawing," *Nanoscale*, vol. 6, no. 9, pp. 4889–4895, 2014.

[22] Q. Waheed, A. N. Khan, and R. Jan, "Investigating the reinforcement effect of few layer graphene and multi-walled carbon nanotubes in acrylonitrile-butadiene-styrene," *Polymer (United Kingdom)*, vol. 97, pp. 496–503, 2016.

[23] A. N. Khan, Q. Waheed, R. Jan, K. Yaqoob, Z. Ali, and I. H. Gul, "Experimental and theoretical correlation of reinforcement trends in acrylonitrile butadiene styrene/single-walled carbon nanotubes hybrid composites," *Polymer Composites*, 2017.